Classification of Limit Solutions of a Mean-Field Oscillator Ising Model

Abstract

Oscillator Ising Machines (OIMs) have become popular tools for solving combinatorial optimization problems and have also recently been investigated for use in associative memory applications. In this article, we study the mean-field limit of OIMs using techniques from gradient flows and the calculus of variations. We provide a complete classification of limit solutions of this model. In particular, all limit solutions are fixed points with phases clustered into at most four groups. For almost all parameter values, only fixed points with clusters at 0 and/or π can be stable. We give tight bounds on the parameter thresholds for which these configurations are stable, thereby identifying the so-called "threshold for binarization" in this model.

1 Introduction

Combinatorial Optimization Problems (COPs) are a cornerstone of modern technology, with examples including resource allocation, network routing, and data compression. Many of these problems are NP-complete, and as the size of these problems grows, the computational resources and time required to obtain solutions increase exponentially. As a potential solution, there has been a resurgence of interest in using alternative computing paradigms as opposed to traditional Von Neumann-based architectures. The Ising problem is the problem of finding spins $\sigma_i \in \{-1, 1\}$ that minimizes the Ising Hamiltonian $H(\sigma) = \frac{1}{2}\sum_{i,j=1}^{N} A_{ij}\sigma_i\sigma_j$, where A_{ij} is the connection strength between nodes i and j. Minimizing the Ising Hamiltonian encourages the spins to align when there is a negative connection between them, and vice versa. The N spins σ_i can be interpreted in multiple ways, as magnetic spins in Ising's original formulation, graph partitions in MaxCut problems, etc. As shown in [1], the reformulation of various NP-complete COPs (thereby all 21 of Karp's equivalent NP-complete problems [2]) results in minimizing the Ising Hamiltonian. These alternate computing paradigms perform gradient descent using a surrogate energy function whose minima coincide with those of the Ising problem. Replicating these gradient systems on physical hardware, such as FPGAs ([3]) and optical lasers ([4]), results in a coupled nonlinear system also known as an Ising machine.

Among the various flavors of IMs, coupled-oscillator-based Oscillator Ising Machines (OIMs) have been highly successful in providing state-of-the-art solutions in a fast, energy-efficient, and scalable manner. First introduced in [5] and [6], OIMs are parameterized dynamical systems given by (1)

$$\dot{\theta}_i = \sum_{j=1}^{N} A_{ij}\sin(\theta_i - \theta_j) - K_s\sin(2\theta_i) \tag{1}$$

where A_{ij} is the edge-weight between node i, j and K_s is known as the second harmonic strength. The OIM consists of two parts: a Kuromoto oscillator to incorporate the coupling in the Ising Hamiltonian. At the same time, the second harmonic injection aims to force the oscillators to take on binary values in $\{0, \pi\}$. Given an asymptotically stable equilibrium point $\theta \in \{0, \pi\}^N$ of (1), a read-out of $\sigma_i = \cos(\theta_i) \in \{-1, 1\}$ returns back the spin configuration. In the decades following its proposal, experimental investigations of OIMs have revealed best practices and trade-offs for efficiently obtaining optimal solutions, as documented in [7] and [8]. On the theoretical side, the authors of [9] classify the equilibrium points of (1) for an arbitrary graph connectivity. However, this classification does not extend very far as it is not possible to enumerate all equilibrium points of (1) in closed form. Furthermore, this prevents them from conducting a comprehensive stability analysis of the equilibrium points. To

overcome this limitation, we begin with an all-to-all connected graph and discuss the equilibrium points and their stability in the limit of infinite oscillators of the following normalized OIM

$$\dot{\theta}_i = \frac{1}{N}\sum_{j=1}^{N} A_{ij}\sin(\theta_i - \theta_j) - K_s \sin(2\theta_i). \tag{2}$$

To discuss the limiting mean-field model of (2), we borrow techniques from the analysis of the infinite-dimensional Kuramoto model. The Kuramoto model was first proposed in [10] and has garnered considerable attention due to its applications in synchronization, power networks, and neuroscience, among other fields. The works of [10] and [11] successfully employ mean-field methods to obtain estimates on the critical coupling strength for synchronization in the Kuramoto model. The authors refer readers to the works of [12] and [13] for a comprehensive review of the infinite-dimensional all-to-all connected Kuramoto model. The classical results of the critical coupling strength and bifurcation analysis have been performed for non-local coupling and graph limits in [14], [15], and [16]. The mathematical machinery presented in [10],[13] have been utilized to analyze the infinite-dimensional OIMs in this article.

The main contributions of this article are as follows.

- Firstly, we formalize the mean-field limit of the model in both the Lagrangian and Eulerian interpretations and demonstrate the equivalence between the two.
- Secondly, we compute all the equilibrium distributions of the mean-field model along with their stability. We show that for almost all parameter values, stable configurations must have mass distributions supported in $\{0, \pi\}$.
- Thirdly, we give tight bounds on the parameter thresholds for which the above configurations are stable. Using these results, we can characterize the threshold of binarization for the Erdos-Reyni graphs, which match numerical predictions.

The rest of the paper is organized as follows. In Section 2, we formulate the problem of interest. Next, we present the main results in Section 3, which include the equilibrium, stability analysis, and bounds on parameter thresholds. Based on the results obtained, we analyze the threshold for binarizing OIMs defined on Erdős-Rényi graphs in Section 4. In Section 5, we provide numerical results to validate our theoretical results, and conclude with our conclusions and future work in Section 6.

2 Problem Formulation

Many combinatorial optimization problems can be recast as minimization problems of the following form [1]

$$\min_{\sigma\in\Sigma} \ \frac{1}{2}\sum_{i,j} A_{ij}\sigma_i\sigma_j. \tag{3}$$

Here, i, j are discrete indices taking values in the index set $\{1, ..., N\}$, the optimization variable σ is a vertex of the N-dimensional hypercube $\Sigma = \{\pm 1\}^N$, and A is a symmetric weight matrix with real entries. The function being minimized in (3) is sometimes referred to as the *Ising Hamiltonian* and the optimization variable σ is sometimes called a *spin configuration.*

Many approaches to solving (or finding approximate solutions to) this problem involve embedding the above (discrete) problem into a continuous minimization problem having the same minimizers and then applying some

sort of continuous optimization algorithm such as gradient descent. A popular way to embed the above problem is using *Kuramoto oscillators* with *second-harmonic injection*

$$\min_{\theta \in \mathbb{T}^N} \ \frac{1}{2N} \sum_{i,j} A_{ij} \cos(\theta_i - \theta_j) - \frac{K_s}{2} \sum_i \cos(2\theta_i). \tag{4}$$

Here, the optimization variable θ is now a continuous variable in the N-torus $\mathbb{T}^N$. The first term takes the same value as the Ising Hamiltonian when $\sigma_i = \cos(\theta_i)$ and $\theta \in \{0, \pi\}^N$. The second term (the "second-harmonic injection") incentivizes θ to take values in this set. The parameter $K_s > 0$ controls the relative strength of this incentivization. Gradient descent on this cost function then yields the dynamics

$$\dot{\theta}_i \ = \ \frac{1}{N} \sum_j A_{ij} \sin(\theta_i - \theta_j) - K_s \sin(2\theta_i). \tag{5}$$

In this paper, we study the *mean-field limit* of these dynamics, i.e., the $N \to \infty$ limit when $A_{ij} \equiv K$ is taken as the "average connectivity" in the network. We allow K to take any value in $\mathbb{R}$. In particular, $K > 0$ corresponds to the case of *repulsive* oscillators, while $K < 0$ corresponds to the case of *attractive* oscillators. Both cases are of interest and are treated in this paper.

2.1 Derivation of Continuum Model

Here, we provide a formal derivation of two different representations of the mean-field limit of the dynamics (5), which we refer to as *Lagrangian* and *Eulerian* representations in analogy with fluid mechanics.

The Lagrangian representation describes the dynamics in terms of the phases of individual oscillators, and is derived by passing directly from the discrete index i to a continuum index x in (5). We first normalize the index set as well as the Ising Hamiltonian by $\frac{1}{N}$, and then pass to the limit to obtain the continuum energy function

$$E(\theta) \ = \ \frac{K}{2} \iint \cos\left(\theta(x) - \theta(y)\right) \mathrm{d}x \, \mathrm{d}y - \frac{K_s}{2} \int \cos(2\theta(x)) \, \mathrm{d}x \tag{6}$$

and corresponding dynamics

$$\dot{\theta}(x) \ = \ K \int \sin(\theta(x) - \theta(y)) \, d\mathrm{d}y - K_s \sin(2\theta(x)). \tag{7}$$

Here, the indices x, y are now continuous variables valued in the index set $[0,1]$. The state variable θ is now a function from the index set $[0,1] \to \mathbb{T}$ which we call the *phase function*, and all integrals occur over the index set $[0,1]$. (θ is assumed to be measurable, and so both the energy (6) and dynamics (7) are well-defined.)

While the Lagrangian representation is perfectly adequate to describe the dynamics of the system, the symmetry of the agents in the mean-field model results in an inherent extraneity in this representation. In words, since any two agents should be "interchangeable", the dynamics of the system should be well-defined independently of any indexing. Indeed, by pushing forward both the phases and dynamics from the index set $[0,1]$ to the torus $\mathbb{T}$, we can obtain a representation (the *Eulerian* representation) which is independent of any index set.

The phases and dynamics push forward differently, as we now explain. First, the phases push forward from a *phase function* $\theta : [0,1] \to \mathbb{T}$ to a *phase density* $\rho : \mathbb{T} \to \mathbb{R}$. Specifically, ρ is the density on $\mathbb{T}$ formed by pushing the uniform density $\mathbb{1}$ on the index set $[0,1]$ forward through the phase function $\theta : [0,1] \to \mathbb{T}$. Thus, the quantity[1]

[1]We note that there is an overloading of notation here in that θ is being used both for the phase function $\theta : [0,1] \to \mathbb{T}$ and for the independent spatial variable $\theta \in \mathbb{T}$. This is useful since the phase of an oscillator is then always denoted θ, but we point this out so as not to confuse the reader.

$\rho(\theta)$ describes the relative density of oscillators with phase $\theta \in \mathbb{T}$. This operation of (density) pushforward is written abstractly as $\rho = \theta_{\#}\mathbb{1}$. Mathematically, this just means that

$$\int_A \rho(\theta)\,\mathrm{d}\theta \;=\; \int_{\theta^{-1}(A)} 1\,\mathrm{d}x \tag{8}$$

for all $A \subset \mathbb{T}$ measurable, or equivalently, that

$$\int_{\mathbb{T}} f(\theta)\rho(\theta)\,\mathrm{d}\theta \;=\; \int_{[0,1]} f(\theta(x))\,\mathrm{d}x \tag{9}$$

for all $f : [0,1] \to \mathbb{T}$ measurable. It is worth pointing out that this operation of density pushforward is defined so as to conserve mass. In particular, since $\mathbb{1}$ is a probability density (i.e. it is nonnegative with total mass 1), ρ is a probability density as well. It is also worth pointing out that in general ρ may have *discrete* components – that is, Dirac masses – if θ has level sets with nonzero measure.

The dynamics, on the other hand, push forward according to a different principle. They push forward as a *function* (rather than as a density), which conserves the *value* (rather than the mass). In particular, the dynamics in the Lagrangian representation take the form of an *assignment* $F : [0,1] \times \mathbb{T} \to \mathbb{R},\ (x, \theta(x)) \mapsto \dot{\theta}(x)$. Importantly, F depends only on the phase $\theta(x)$ (not on the particular index x), and so F factors over $\mathbb{T}$ to yield a vector field

$$v_\theta \;:\; \mathbb{T} \;\to\; \mathbb{R} \tag{10}$$

$$\bullet \;\mapsto\; K\int_{[0,1]} \sin(\bullet - \theta(y))\,\mathrm{d}y - K_s\sin(2\bullet). \tag{11}$$

The integral term can then be pushed forward from $[0,1]$ to $\mathbb{T}$ using the rule (9) to obtain:

$$v_\rho \;:\; \mathbb{T} \;\to\; \mathbb{R} \tag{12}$$

$$\bullet \;\mapsto\; K\int_{\mathbb{T}} \sin(\bullet - \theta')\,\rho(\theta')\,\mathrm{d}\theta' - K_s\sin(2\bullet). \tag{13}$$

The density ρ then evolves according to the *continuity equation*

$$\dot{\rho}(\theta) \;=\; -\nabla\cdot(v_\rho(\theta)\,\rho(\theta)), \tag{14}$$

which describes the transport of ρ by the vector field v_ρ under conservation of mass. (In the above, $\nabla\cdot$ denotes the divergence operator.) Thus, the dynamics in the Eulerian setting are given by the equation

$$\dot{\rho}(\theta) \;=\; -\nabla\cdot\left(\left[K\int_{\mathbb{T}} \sin(\theta-\theta')\,\rho(\theta')\,d\theta' - K_s\sin(2\theta)\right]\,\rho(\theta)\right). \tag{15}$$

We remark that there are several equivalent ways that we could have derived the dynamics (15). Here, we took the route: Ising Hamiltonian → gradient flow dynamics → continuum limit → representation over $\mathbb{T}$. However, these steps could have been carried out in any order. In particular, there exist both discrete and continuum counterparts over both the index set and $\mathbb{T}$ for all of the objects discussed above, as well as appropriate notions of gradient flows in each of these settings. (In particular, the appropriate notion of gradient flow for energy functions of densities over $\mathbb{T}$ is given by the so-called *Wasserstein gradient flow* [17], but we will not expand upon this here.)

Both Lagrangian and Eulerian formulations are useful, but for different reasons. The Lagrangian formulation is more flexible, but more complicated, whereas the Eulerian formulation deals with simpler objects, but is poorly suited for certain analyses. This is a theme that runs throughout the paper.

The last comment we make here is that this derivation reveals that the existence of an Eulerian representation for these models is highly dependent on the symmetries of the agents and the resulting factorability of F. In particular, while a phase density ρ is always defined, it does not always provide a sufficient statistic for the evolution of the system. The dynamics of the system can be written as a PDE for a single density as in (15) if and only if F factors over $\mathbb{T}$, as in when all agents are symmetric. If there are N species of agents such that all agents within a given species are symmetric, then F factors over $\{1, ..., N\} \times \mathbb{T}$, and we may obtain a coupled system of N PDEs for the densities of each species. If agents are all asymmetric so that F does not factor, then the Lagrangian representation is in general the best we can do.

2.2 Problem Statement

The problem that we study in this paper is the following: *characterize all limit solutions of the model* (7) *(equivalently,* (15)*) and their stability.*

This is carried out in the next section. In particular, we show that:

- All limit solutions are fixed points.
- At these fixed points, the phases cluster into at most four groups.
- For almost all parameter values K/K_s, only fixed points with clusters at 0 and/or π can be stable.
- A fixed point with clusters at 0 and/or π is stable only for a very specific range of parameter values K/K_s.

3 Main Results

In this section, we carry out the analysis of the limit solutions of the models (7), (15) and their stability. Our analysis is based largely on tools from gradient flows and the calculus of variations. Thus, we begin by describing the gradient flow structure of this system.

3.1 Gradient Flow Structure

First, we verify that the continuum dynamics (7) are indeed the gradient flow dynamics of the continuum energy (6). However, since the state space $\Theta := \{\theta : [0,1] \to \mathbb{T}\}$ is not only infinite-dimensional, but not even a vector space, we need to be careful about what exactly we mean by "gradient flow".

To make this rigorous, we identify Θ with the L^2 space of functions $[0,1] \to \mathbb{R}$ with values identified modulo 2π. This makes Θ into a Hilbert manifold, i.e., an infinite-dimensional Riemannian manifold which is modeled locally on a Hilbert space. The tangent (Hilbert) spaces are all identified with $L^2([0,1];\mathbb{R})$, and inherit the standard L^2 inner product $\langle \cdot, \cdot \rangle$. Importantly, this makes Θ a flat space, and so we can work in local coordinates, taking derivatives just as we would in L^2.

The energy function (6) is very nice. In particular, it is smooth with respect to the L^2 structure on Θ defined above, admitting bounded derivatives of all orders. We can use this to define the gradient flow as follows. First, let $DE(\theta)$ denote the Frechet differential or first variation of E at the point θ (which is well-defined since E is smooth). The Riemannian structure of Θ then allows us to define the gradient $\nabla E(\theta)$ as the Riesz representation of DE, that is, $\langle \nabla E(\theta), p \rangle = DE(\theta)[p]$ for all $p \in L^2([0,1];\mathbb{R})$. Then, we may write the gradient flow as $\dot{\theta} = -\nabla E(\theta)$ with no ambiguity as to what is meant.

The smoothness of E also implies that the gradient vector field $-\nabla E$ is Lipschitz, and so by the Picard-Lindelof Theorem, we obtain global well-posedness of the gradient flow dynamics. The inherent locality of the dynamics together with the flatness of Θ also allow us to characterize fixed points and their stability in terms of the gradient ∇E and Hessian $\nabla^2 E$ just as we would in L^2.

We state all of these results in the following Lemmas.

Lemma 1. *The dynamics* (7) *are the gradient flow dynamics of the energy* (6) *with respect to the L^2 structure on $\Theta := \{\theta : [0,1] \to \mathbb{T}\}$ defined above.*

Proof. We first expand E around a curve $\theta(t)$ to obtain

$$E(\theta(t)) \;=\; E(\theta(0)) + tDE(\theta(0))[\dot{\theta}(0)] + o(t), \tag{16}$$

where DE denotes the Frechet differential or first variation. The time derivative of $E(\theta(t))$ at $t = 0$ is then $\dot{E}(\theta(0)) = DE(\theta(0))[\dot{\theta}(0)]$. Let ∇E denote the Riesz representation of the differential DE (i.e. the gradient) and $\langle \cdot, \cdot \rangle$ the L^2 scalar product, so that we may write

$$\dot{E}(\theta(0)) \;=\; \langle \nabla E(\theta(0)), \dot{\theta}(0) \rangle. \tag{17}$$

We can then see immediately that θ is the gradient flow of E if it satisfies

$$\dot{\theta} \;=\; -\nabla E(\theta). \tag{18}$$

We may compute the first variation DE by the usual method (i.e. perturb theta, consider terms which are first-order in the perturbation) to find

$$DE(\theta)[\dot{\theta}] \;=\; -\frac{K}{2} \int \int \sin(\theta(x) - \theta(y)) \left(\dot{\theta}(x) - \dot{\theta}(y)\right) \mathrm{d}x \, \mathrm{d}y + K_s \int \sin(2\theta(x)) \, \dot{\theta}(x) \, \mathrm{d}x. \tag{19}$$

Using a change of variables to turn the $\dot{\theta}(y)$ into a $\dot{\theta}(x)$, we can then isolate $\dot{\theta}(x)$ to find that

$$\nabla E(\theta)(x) \;=\; -K \int \sin(\theta(x) - \theta(y)) \, \mathrm{d}y + K_s \sin(2\theta(x)). \tag{20}$$

The gradient flow dynamics are then given by

$$\dot{\theta}(x) \;=\; -\nabla E(\theta)(x) \;=\; K \int \sin(\theta(x) - \theta(y)) \, \mathrm{d}y - K_s \sin(2\theta(x)), \tag{21}$$

exactly as in (7). ∎

Lemma 2. *The gradient flow dynamics* (7) *are globally well-defined.*

Proof. We compute the second variation by the usual method (i.e., expand $E(\theta(t,s))$ around a function $\theta(t,s) = \theta(0) + tp + sq$, and consider terms which are bilinear in t, s) to obtain

$$D^2 E(\theta)[p,q] \;=\; \int \left(2K_s \cos(2\theta(x)) - K \int \cos(\theta(x) - \theta(y)) \, \mathrm{d}y \right) p(x) q(x) \, \mathrm{d}x \\ + K \iint \cos(\theta(x) - \theta(y)) p(y) q(x) \, \mathrm{d}y \, \mathrm{d}x. \tag{22}$$

It is easily seen that this is a bounded bilinear operator, thus the gradient vector field $-\nabla E$ is Lipschitz, and so by the Picard-Lindelof Theorem, the dynamics are globally well-posed. ∎

Lemma 3. *A point $\theta \in \Theta$ is a fixed point of the gradient flow dynamics* (7) *if and only if* $\nabla E(\theta) = 0$.

Proof. Follows immediately from the definition of the gradient flow dynamics $\dot{\theta} = -\nabla E(\theta)$. ■

A nice feature of gradient flows is that the energy function E is automatically a Lyapunov function, with trajectories satisfying a certain *Energy Dissipation Equality* (EDE).

Lemma 4. *Let $\theta(t)$ denote any trajectory of the dynamics* (7). *Then $E(\theta(t))$ satisfies the following* Energy Dissipation Equality *(EDE)*

$$\dot{E}(\theta(t)) \;=\; -\|\nabla E(\theta(t))\|_{L^2}^2. \tag{23}$$

Proof. The result can be obtained immediately from substituting (18) into (17). ■

This is useful both for characterizing the stability of fixed points and in constraining the behavior that can occur in these systems.

Lemma 5. *For a fixed point $\theta \in \Theta$ to be asymptotically stable, it is necessary that $\nabla^2 E(\theta) \geq 0$ and sufficient that $\nabla^2 E(\theta) > 0$, where $\nabla^2 E$ denotes the Hessian of E (i.e. the Riesz representation of the second variation $D^2 E$).*

Proof. To show necessity, observe that if $\nabla^2 E(\theta) < 0$, then there exists a direction p such that $D^2 E(\theta)[p,p] < 0$. Taylor expanding E around θ yields

$$E(\theta + \epsilon p) \;=\; E(\theta) + \epsilon DE(\theta)[p] + \frac{\epsilon^2}{2} D^2 E(\theta)[p,p] + o(t^2). \tag{24}$$

The linear term vanishes since θ is a fixed point, and therefore, for sufficiently small ϵ, $E(\theta + \epsilon p) < E(\theta)$. Denote by $\theta_\epsilon(t)$ the trajectory of (7) starting from $\theta + \epsilon p$. The EDE (23) ensures that $E(\theta_\epsilon(t))$ is nonincreasing, thus by the continuity of E, $\theta_\epsilon(t)$ remains bounded away from θ, and so θ cannot be asymptotically stable.

On the other hand, to show sufficiency, observe that by the same arguments, if $\nabla^2 E > 0$, then E forms a local Lyapunov function for the fixed point θ. ■

Lemma 6. *The limit set of any trajectory of* (7) *is contained in the set of fixed points of* (7).

Proof. By the Lasalle Invariance Principle and the EDE (23), the limit sets of any trajectory of (7) are contained in the set

$$\{\theta \in \Theta \;:\; \dot{E}(\theta) = -\|\nabla E(\theta)\|^2 = -\|\dot{x}\|^2 = 0\}, \tag{25}$$

that is, the set of fixed points of (7). ■

Note that while the limit set of any trajectory is *contained* in the set of fixed points, this does not necessarily imply that every trajectory *converges to a fixed point.* To show this, we require stronger arguments.

To be completed...

We remark that all of the above results translate to the Eulerian representation as well, except that the correct notion of gradient flow in that case is a *Wasserstein gradient flow* [17]. However, we will not elaborate this point here.

3.2 First-Order Analysis: Equilibria

From our earlier analysis, the following result is immediate.

Lemma 7. *A point $\theta \in \Theta$ is a fixed point of the system (7) if and only if for (almost) all $x \in [0,1]$, $\theta(x)$ is valued in the zero set of the velocity field*

$$v_\theta(\bullet) \;=\; K \int_{[0,1]} \sin(\bullet - \theta(y))\, \mathrm{d}y - K_s \sin(2\bullet). \tag{26}$$

Proof. Follows directly by applying the specific form for ∇E derived in the proof of Lemma 1 to Lemma 5. ∎

In the Eulerian setting, this statement translates to the following.

Corollary 8. *A point $\rho \in P$ is a fixed point of the system (15) if and only if ρ is supported on the zero set of the velocity field*

$$v_\rho(\bullet) \;=\; K \int_{\mathbb{T}} \sin(\bullet - \theta')\, \rho(\theta')\, \mathrm{d}\theta' - K_s \sin(2\bullet). \tag{27}$$

Proof. By the pushforward relation (ref), θ is valued in a set $A \subset \mathbb{T}$ for (almost) all x if and only if ρ has support contained in A. ∎

In the above, P denotes the space of probability densities on $\mathbb{T}$, i.e., the state space in the Eulerian representation.

In the next section, we explore the structure of the velocity field v. It turns out that v is a highly structured object (for example, it has a finite number of isolated zeros), which makes it possible to compute all equilibrium configurations of the system.

3.3 Structure of Vector Fields

Here, we examine the structure of v and its zero set in more depth. Consider the Eulerian representation

$$v_\rho(\theta) \;=\; K \int_{\mathbb{T}} \sin(\theta - \theta')\, \rho(\theta')\, \mathrm{d}\theta' - K_s \sin(2\theta). \tag{28}$$

We can see that the integral term takes the form of a convolution so that we can also write v more compactly as

$$v_\rho \;=\; K \sin * \rho - K_s \sin(2\bullet). \tag{29}$$

Since v depends on ρ only through the term $\sin * \rho$, which itself only depends on the *first harmonic* of ρ, we can reparameterize v in terms of this first harmonic (sometimes also called the *order parameter*). This is well known.

Lemma 3.0.1. The vector field (28) can be equivalently written in either of the forms

$$\begin{aligned} v_z(\theta) \;&=\; -K \operatorname{Im}[z e^{-i\theta}] - K_s \sin(2\theta) && (30)\\ &=\; -K|z| \sin(\angle z - \theta) - K_s \sin(2\theta), && (31) \end{aligned}$$

where

$$z \;=\; z_\rho \;:=\; \int_{\mathbb{T}} \rho(\theta)\, e^{i\theta}\, \mathrm{d}\theta \tag{32}$$

is the complex *order parameter* of the system, having magnitude $|z|$ and phase $\angle z$.

Proof. Define the order parameter z as in (32), and then rewrite the vector field as follows

$$\begin{aligned} v(\theta) &= K \int \sin(\theta - \theta')\, \rho(\theta')\, \mathrm{d}\theta' - K_s \sin(2\theta) \\ &= -K \int \mathrm{Im}\left[e^{-i\theta} e^{i\theta'}\right] \rho(\theta')\, \mathrm{d}\theta' - K_s \sin(2\theta) \\ &= -K\, \mathrm{Im}\left[\int \rho(\theta') e^{i\theta'} \mathrm{d}\theta'\ e^{-i\theta}\right] - K_s \sin(2\theta) \\ &= -K\, \mathrm{Im}[z e^{-i\theta}] - K_s \sin(2\theta). \end{aligned}$$

If the order parameter is written in polar form as $z = |z| e^{i \angle z}$, then the velocity field becomes

$$v(\theta) = -K|z| \sin(\angle z - \theta) - K_s \sin(2\theta). \tag{33}$$

■

If the density ρ is represented as a density over the unit circle in the complex plane, then the order parameter z can be interpreted as the (complex) center of mass of ρ. Of course, z can also be expressed in terms of the phase function θ rather than the phase density ρ using the rule (9).

There are several important conclusions that can be drawn from this reparameterization of v:

1. v depends on ρ only through its dependence on z_ρ.
2. In particular, v can be finitely parameterized using just two real variables (in addition to K, K_s).
3. v is analytic.
4. In particular, v has a finite number of isolated zeros (2, 3, or 4, as will be shown later).

In particular, since a density ρ must be supported on the zero set of v in order to be an equilibrium point, all equilibria must be discrete densities (i.e. sums of Dirac masses) with at most 4 components.

Moreover, this finite parameterization of v makes it relatively easy to search over possible zero sets, and thus possible equilibrium configurations of ρ. Essentially, we can first write the condition that ρ be supported on the zero set of v_ρ as $v_\rho \rho = 0$ (which can be made rigorous in either a measure-theoretic or distributional sense). We can then rewrite this condition in terms of z as two separate conditions: $v_z \rho = 0$ and $z = z_\rho$. The first condition is satisfied if and only if ρ is supported on the zero set of v_z. The second condition is satisfied if and only if z is the complex center of mass of ρ. In turn, given some z which defines the vector field v_z, it is possible to construct a ρ that simultaneously satisfies these two conditions if and only if z belongs to the convex hull of the zero set of v_z. Furthermore, if this holds, then any such ρ will be a fixed point.

Lemma 9. *Given z, K, K_s, consider the velocity field $v = v_z$ as defined in* (3.4)*. Then:*

1. *There exists a ρ such that $v_\rho \rho = 0$ if and only if z lies in the convex hull of the zero set of v_z.*
2. *Supposing (1) holds, then every such ρ takes the form $\rho = \sum_i m_i \delta_{z_i}$ for some convex coefficients $\{m_i\}$ of z: $z = \sum_i m_i z_i$, $\sum_i m_i = 1$, $m_i \geq 0$, and where $\{z_i\}$ denotes the zero set of v.*

Proof. It should be clear that ρ satisfies $v_\rho \rho = 0$ if and only if it simultaneously satisfies $v_z \rho = 0$ and $z = z_\rho$ if and only if ρ is simultaneously supported on the zero set of v_z and has z as its complex center of mass. We claim that there exists a ρ simultaneously satisfying these conditions if and only if z belongs to the convex hull of the zero set of v_z.

To show the forward direction, suppose there exists such a ρ. Then its center of mass z is contained in the convex hull of its support which in turn is contained in the convex hull of the zero set of v_z, since ρ is supported in the zero set of v_z.

To show the reverse direction, suppose that z belongs to the convex hull of the zero set of v_z, which we denote $\{z_i\}$. Then there exist convex coefficients m_i such that $z = \sum_i m_i z_i$, $m_i \geq 0$, $\sum_i m_i = 1$. It is immediate to verify that any $\rho = \sum_i m_i \delta_{z_i}$ satisfies both $v_z \rho = 0$ and $z = z_\rho$. Furthermore, all ρ satisfying these conditions must be of this form for some $\{m_i\}$, since 1) ρ is a probability density supported on the zero set of v_z if and only if $\rho = \sum_i m_i \delta_{z_i}$ for some convex coefficients $\{m_i\}$, and 2) z is the center of mass of ρ if and only if $z = \sum_i m_i z_i$. ■

This suggests the following approach to identifying all equilibria of the system:

1. Sweep over the parameter space z, K, K_s to identify all possible velocity fields v_z.
2. For each velocity field v_z, compute its zero set, and check whether z is contained in the convex hull.
3. If z is contained in the convex hull, find the sets of convex coefficients $\{m_i\}$ for which $z = \sum_i m_i z_i$.
4. Any ρ of the form $\rho = \sum_i m_i \delta_{z_i}$ will then be an equilibrium point of the system.

We may also leverage symmetries of the system to reduce the number of parameters that we need to search over as follows. Starting with the system in the form

$$\dot{\rho}_t \;=\; -\nabla \cdot (v_{\rho_t}\, \rho_t) \tag{34}$$

(i.e. explicitly including the time-dependence), observe that this system has the following time-scaling symmetry: (ρ_t, v_{ρ_t}) is a solution to (34) if and only if $(\rho_{\alpha t}, \alpha v_{\rho_{\alpha t}})$ is a solution. This scaling holds for all nonzero $\alpha \in \mathbb{R}$. In other words, we can consider scalings of the vector field v to be equivalent to scalings of time. In particular, ρ is a fixed point for the velocity field v_ρ if and only if it is a fixed point for the velocity field αv_ρ. Furthermore, if $\alpha > 0$, then the direction of time – and thus also the stability of rho – is preserved.

This justifies studying fixed points only for the normalized velocity fields

$$\tilde{v}_z(\theta) \;:=\; -\frac{K}{K_s}|z|\sin(\angle z - \theta) - \sin(2\theta). \tag{35}$$

(Note that K_s is assumed to be strictly > 0.) We thus only need to search over the three-parameter[2] space $(K/K_s, |z|, \angle z)$ to identify all possible equilibrium points and their stability. In the next section, we carry out this enumeration of equilibria.

3.4 Enumeration of Equilibria

In this subsection, we discuss the number of zeros of the normalized velocity field (35).

Lemma 3.0.2. Given a stationary distribution ρ, there exists exactly two, three or four zeros of the corresponding velocity field given by (35).

Proof. Given the stationary distribution ρ the velocity field can be written as

$$\bar{v}_z(\theta) = -A\sin(\angle z - \theta) - \sin(2\theta) \tag{36}$$

$$= -A\sin(\angle z)\cos(\theta) + A\sin(\theta)\cos(\angle z) - 2\sin(\theta)\cos(\theta) \tag{37}$$

[2]Note that while the *zero-sets* of v can be parameterized using just two parameters $K|z|/K_s$ and $\angle z$, whether or not these zero sets actually correspond to *equilibria* depends on the value of $|z|$, thus three parameters are required for the identification of equilibria.

Rewriting the velocity field by we can write $v(\theta) = a\cos\theta + b\sin\theta - 2\sin\theta\cos\theta$, where $a = -A\sin(\angle z), b = A\cos(\angle z)$. Associated with the velocity field, we can define the following two conics $H_1 \equiv ax + by - 2xy = 0$ and $C_1 \equiv x^2 + y^2 - 1 = 0$. Then the zeros of the velocity field $v(\theta)$ are exactly the points of intersection of the two conics C_1, H_1. By applying Bézout's theorem, we can conclude that the two conics can intersect at-most at four points. Additionally, we note that the hyperbola H_1 always passes through the origin, therefore for all a, b, the curves C_1 and H_1 intersect in at-least two points. Therefore, there exists exactly two, three or four zeros of the velocity field . ■

We have shown that there are exactly two, three or four intersection points, next we have to crosscheck if it is possible for the center of mass of the distribution can lie in the convex hull of the intersection points. We notice that the center of mass is given by $z = (K_s b/K, -K_s a/K)$ and therefore lies on the line $y = -(a/b)x$. Additionally, the tangent to the hyperbola at the origin is given by $y = (-a/b)x$. If the hyperbola intersects the circle at exactly two points, the line joining the points of intersection and the tangent at the origin will never intersect inside the circle, as demonstrated in Figure 1:(a).

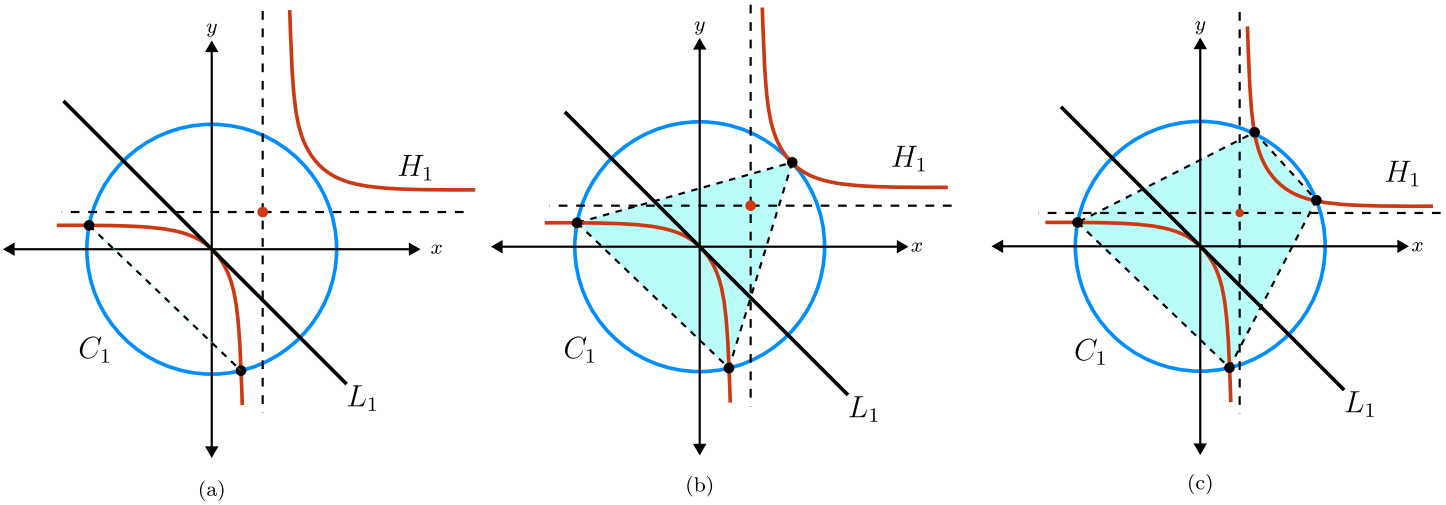

Figure 1: Diagrammatic description of the three cases between the intersection of the hyperbola $H_1 \equiv ax + by - 2xy = 0$ and the unit circle $C_1 \equiv x^2 + y^2 - 1 = 0$; (a) two points of intersection, (b)three points of intersection, (c) four points of intersection. The red point denotes the center of the hyperbola given by $(b/2, a/2)$, the black dots denote the points of intersection between C_1, H_1. The black line $L_1 \equiv y + (a/b)x = 0$ is the tangent to H_1 at the origin, that also contains complex order parameter z visualized as a point in $\mathbb{R}^2$. The shaded region in cyan denotes the convex-hull formed by the points of intersection.

We can see that if the hyperbola and the unit circle intersect at three or four points, then there always exists a non-empty convex hull. We have the following compatibility conditions

- For the hyperbola H_1 to intersect the unit circle C_1 at three or four points, the parameters a, b must satisfy $a^{2/3} + b^{2/3} \leq 2^{2/3}$ as shown in Appendix A
- The complex order parameter z must satisfy $|z| \leq 1$. Therefore, we can conclude that $a^2 + b^2 \leq (K/K_s)^2$
- Additionally, density ρ supported on the zeros of $\bar{v}_z(\theta)$ must be compatible with z, i.e. $\int \rho(\theta) e^{i\theta} \mathrm{d}\theta = z$.

Therefore we can give the following class of probability measures on the unit circle parameterized by a, b for

densities that have three or four distance support points

$$\rho \in \Bigg\{ \sum_{i=1}^4 m_i \delta_{\theta_i} \;\Bigg|\; \theta_i \in [0, 2\pi], a\cos(\theta_i) + b\sin(\theta_i) = \sin(2\theta_i), \text{ at least three distinct } \theta_i \\ m_i \geq 0, \sum_{i=1}^4 m_i = 1, \sum_{i=1}^4 m_i \cos(\theta_i) = bK/K_s, \sum_{i=1}^4 m_i \sin(\theta_i) = -aK/K_s, \\ a^2 + b^2 \leq \left(K/K_s\right)^2, \\ a^{2/3} + b^{2/3} < 2^{2/3} \Bigg\}. \tag{38}$$

3.5 Second-Order Analysis: Stability

To investigate the stability of equilibria, we rely on the second-order conditions given in Lemma (5): for a fixed point θ to be stable, it is necessary that $\nabla^2 E(\theta) \geq 0$ and sufficient that $\nabla^2 E(\theta) > 0$, where $\nabla^2 E$ denotes the Hessian of E.

We return to the Lagrangian representation for this analysis, since the Eulerian representation presents certain difficulties here. Specifically, the Eulerian representation only permits one to perturb equilibria using vector fields, but equilibria are discrete, and such perturbations always preserve their discrete components. However, the physical assumptions underlying our model require us to consider more general perturbations that may break up discrete masses, and this is only possible using the Lagrangian representation.

3.5.1 Necessary Conditions for Stability

The following Lemma is a direct application of Lemma (5) to the particular form for $\nabla^2 E$.

Lemma 10. *For a fixed point θ to be stable, it is necessary (alternatively, sufficient) that the quadratic form*

$$D^2 E(\theta)[p,p] = \int \left(2K_s \cos(2\theta(x)) - K \int \cos(\theta(x) - \theta(y))\, \mathrm{d}y \right) p^2(x)\, \mathrm{d}x \\ + K \iint \cos(\theta(x) - \theta(y)) p(y) p(x)\, \mathrm{d}y\, \mathrm{d}x \tag{39}$$

be positive semi-definite (alternatively, definite). Equivalently, it is necessary (alternatively, sufficient) that the linear operator $\nabla^2 E(\theta)$ be positive semi-definite (alternatively, definite), where $\nabla^2 E(\theta)$ is defined by

$$\left(\nabla^2 E(\theta)[p] \right)(x) = \left(2K_s \cos(2\theta(x)) - K \int \cos(\theta(x) - \theta(y))\, \mathrm{d}y \right) p(x) + K \int \cos(\theta(x) - \theta(y)) p(y)\, \mathrm{d}y. \tag{40}$$

Proof. The proof follows immediately by applying Lemma (5) to the second variation of E. We compute the second variation by the usual method (i.e., expand $E(\theta(t,s))$ around a function $\theta(t,s) = \theta(0) + tp + sq$, and consider terms which are bilinear in t, s) to obtain

$$D^2 E(\theta)[p,q] = \int \left(2K_s \cos(2\theta(x)) - K \int \cos(\theta(x) - \theta(y))\, \mathrm{d}y \right) p(x) q(x)\, \mathrm{d}x \\ + K \iint \cos(\theta(x) - \theta(y)) p(y) q(x)\, \mathrm{d}y\, \mathrm{d}x. \tag{41}$$

Notice that the second variation is by definition a *bilinear form* $D^2E(\theta)[p,q]$. Stability can be determined from positivity of the *quadratic form* $D^2E(\theta)[p,p]$, which is equivalent to positivity of the linear operator/Riesz representation/Hessian $\nabla^2 E(\theta)$, which is defined by $D^2E(\theta)[p,q] = \langle \nabla^2 E(\theta)[p], q\rangle$. ■

These conditions are unwieldy to work with in general. In particular, it is hard to get sufficient conditions out of the quadratic form since it is not possible to isolate p, and thus challenging to find conditions under which the form is positive for all possible p. On the other hand, checking the spectrum of the linear operator involves solving a rather difficult eigenvalue problem.

An alternative approach – and the one we take here – is as follows. While sufficient conditions are relatively hard to derive, necessary conditions are fairly easy. One simply chooses a "nice" perturbation p so that the quadratic form simplifies, and then concludes that any equilibria which are destabilized by p are certainly unstable in general. By finding a clever sequence of perturbations p, one can progressively narrow down the list of "candidate" stable equilibria until (hopefully) all candidate stable equilibria fall into some nice class. Then, one can check sufficient conditions on just that class.

After a lengthy argument involving various symmetries, transformations, cases, and perturbations (all relegated to the appendix), we arrive at the following.

Theorem 11. *For almost all values*[3] *of parameters K/K_s, for a fixed point θ to be stable, it is necessary that it be valued in the set $\{0,\pi\}$.*

Proof. See Appendix B. ■

In the Eulerian setting, this translates to: for almost all values of parameters K/K_s, for a fixed point ρ to be stable, it is necessary that it be supported on $\{0,\pi\}$.

3.5.2 Sufficient Conditions for Stability

We now check sufficient conditions for the stability of phase functions valued in the set $\{0,\pi\}$. We may assume without loss of generality that $\theta(x) = 0$ for $x \in [0,m)$ and $\theta(x) = \pi$ for $x \in (m,1]$. In general, the stability of these configurations depends both on the value of m (i.e. on the relative amount of mass at 0 and π) and on the value of the parameter K/K_s.

Theorem 12. *Let θ be defined by*

$$\theta(x) = \begin{cases} 0 & \text{if } x \in [0,m) \\ \pi & \text{if } x \in (m,1] \end{cases}. \tag{42}$$

Then the following conditions are sufficient for the stability of θ (and necessary if the inequalities are relaxed to be non-strict):

- *If $m \in \{0,1\}$: $K/K_s < 2$.*
- *If $m = 0.5$: $K/K_s > -2$.*
- *If $m \notin \{0, 0.5, 1\}$: $-2/(|2m-1|+1) < K/K_s < 2/|2m-1|$.*

[3]The single remarkable exception happens when $K/K_s = -2$ in the very particular configuration of two masses, each of mass 0.5, at $\theta_1 \in [7\pi/4, \pi/4]$ and $\theta_2 = \pi - \theta_1$. In this case, the equilibria appear to be neutrally stable.

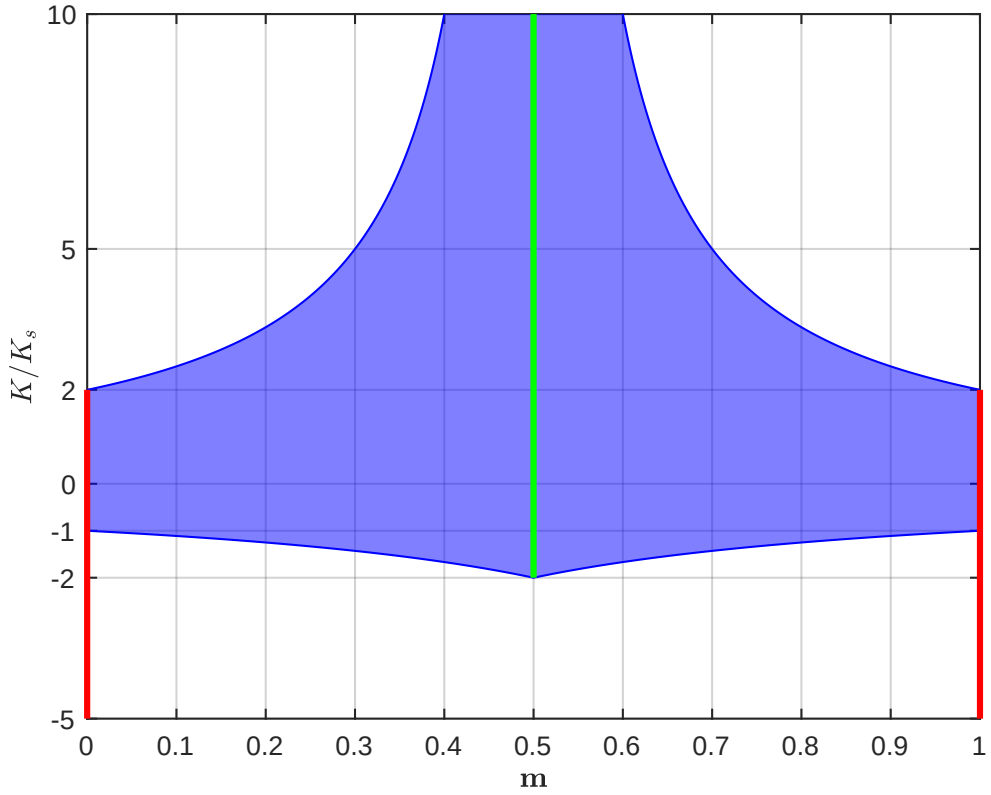

Figure 2: **Stability thresholds for binarized states.** Binarized states are stable for $m \in \{0, 1\}$ when $K/K_s < 2$ (red), for $m = 1/2$ when $K/K_s > -2$ (green), and for $m \notin \{0, 1/2, 1\}$ when $-2/(|2m-1|+1) < K/K_s < 2/|2m-1|$ (blue).

Proof. See Appendix C. ■

This completes the classification of stability of equilibria in this system.

This also identifies the so-called "threshold for binarization" in this system: the "most stable" binarized state is $m_0 = m_\pi = 0.5$, which is stable for $K/K_s > -2$. We may actually identify a few different relevant parameter thresholds:

- *Some* binarized state is stable $\Leftrightarrow$ $K/K_s > -2$.
- *Every* binarized state is stable $\Leftrightarrow$ $-1 \leq K/K_s \leq 2$.
- *Only* binarized states can be stable $\Leftrightarrow$ $K/K_s \geq 2$.

These parameter ranges are depicted graphically in Figure 2.

4 Applications

One of the main aspects of the theoretical and experimental analysis of OIMs is to estimate the second harmonic injection strength required to render the $\{0, \pi\}$ configurations stable. The authors of [9], [7] provide bounds on this

critical value for interested readers. In the case of Erdos-Reyni graphs, where each edge is present or absent with a probability $p \in [0, 1]$, the average of the degree of each node is given by $p(N-1)$. In the case that $N \to \infty$, the parameter K in (7) of the infinite-dimensional OIM is given by $K = p$. From Theorem 12, we can conclude that for $K_s \geq 2p$ every binarized state is stable as $N \to \infty$. Therefore, $K_s^* \sim 2p(N + \mathcal{O}(N))$ as $N \to \infty$. The above estimate motivates further investigation into the infinite-dimensional OIM without the assumption of all-to-all connectedness. To perform such an analysis it is necessary to talk about limit of graph sequences in accordance with the works of [14], [15],[16].

To be completed...

5 Numerical Results

To be completed...

6 Conclusion

In this article, we have analyzed the all-to-all connected infinite-dimensional OIM. By taking the limit $N \to \infty$, we can represent the system in both the Lagrangian and Eulerian frameworks, and we demonstrate their equivalence. Using the Lagrangian representation, we obtain a parameterized representation of the equilibrium densities. We perform linear stability analysis and show that only those densities supported at $\{0, \pi\}$ can be stable. Further, we obtain necessary and sufficient conditions on the parameters of the infinite-dimensional OIM. Using these conditions, we calculate rough estimates of the bounds on the second-harmonic injection strength for Erdős-Rényi graphs. In the future, using the obtained results as a scaffold, the authors would like to address the question of arbitrary graph topologies. In particular, performing rigorous equilibrium and stability analyses on Erdős-Rényi graphs, small-world networks, and power-law networks would be an interesting future direction.

References

[1] Andrew Lucas. “Ising formulations of many NP problems”. In: *Frontiers in Physics* 2 (2014).

[2] Richard M. Karp. “Reducibility Among Combinatorial Problems”. In: *50 Years of Integer Programming 1958-2008*. Springer Berlin Heidelberg, Nov. 2009, pp. 219–241.

[3] Kosuke Tatsumura, Alexander R. Dixon, and Hayato Goto. “FPGA-Based Simulated Bifurcation Machine”. In: *2019 29th International Conference on Field Programmable Logic and Applications (FPL)*. IEEE, Sept. 2019, pp. 59–66.

[4] Shoko Utsunomiya, Kenta Takata, and Yoshihisa Yamamoto. “Mapping of Ising models onto injection-locked laser systems”. In: *Optics Express* 19.19 (Aug. 2011), p. 18091.

[5] Tianshi Wang and Jaijeet Roychowdhury. “OIM: Oscillator-Based Ising Machines for Solving Combinatorial Optimisation Problems”. In: *Unconventional Computation and Natural Computation*. Springer International Publishing, 2019, pp. 232–256.

[6] Tianshi Wang et al. “Solving combinatorial optimisation problems using oscillator based Ising machines”. In: *Natural Computing* 20.2 (May 2021), pp. 287–306.

[7] Mohammad Khairul Bashar, Antik Mallick, and Nikhil Shukla. "Experimental Investigation of the Dynamics of Coupled Oscillators as Ising Machines". In: *IEEE Access* 9 (2021), pp. 148184–148190. ISSN: 2169-3536. DOI: 10.1109/access.2021.3124808. URL: http://dx.doi.org/10.1109/ACCESS.2021.3124808.

[8] A. Mallick et al. "Overcoming the Accuracy vs. Performance Trade-off in Oscillator Ising Machines". In: *2021 IEEE International Electron Devices Meeting (IEDM)*. IEEE, Dec. 2021, pp. 40.2.1–40.2.4. DOI: 10.1109/iedm19574.2021.9720612. URL: http://dx.doi.org/10.1109/IEDM19574.2021.9720612.

[9] Yi Cheng et al. "A control theoretic analysis of oscillator Ising machines". In: *Chaos: An Interdisciplinary Journal of Nonlinear Science* 34.7 (July 2024).

[10] Yoshiki Kuramoto. "Self-entrainment of a population of coupled non-linear oscillators". In: *International Symposium on Mathematical Problems in Theoretical Physics*. Springer-Verlag, pp. 420–422.

[11] Hayato Chiba. "A proof of the Kuramoto conjecture for a bifurcation structure of the infinite-dimensional Kuramoto model". In: *Ergodic Theory and Dynamical Systems* 35.3 (Oct. 2013), pp. 762–834. ISSN: 1469-4417. DOI: 10.1017/etds.2013.68. URL: http://dx.doi.org/10.1017/etds.2013.68.

[12] Juan A. Acebrón et al. "The Kuramoto model: A simple paradigm for synchronization phenomena". In: *Reviews of Modern Physics* 77.1 (Apr. 2005), pp. 137–185.

[13] Steven H. Strogatz. "From Kuramoto to Crawford: exploring the onset of synchronization in populations of coupled oscillators". In: *Physica D: Nonlinear Phenomena* 143.1–4 (Sept. 2000), pp. 1–20.

[14] Yoshiki Kuramoto et al. "Mean-Field Theory Revives in Self-Oscillatory Fields with Non-Local Coupling". In: *Progress of Theoretical Physics Supplement* 161 (2006), pp. 127–143.

[15] Hayato Chiba and Georgi S. Medvedev. "The mean field analysis of the Kuramoto model on graphs I. The mean field equation and transition point formulas". In: *Discrete &; Continuous Dynamical Systems - A* 39.1 (2019), pp. 131–155.

[16] Hayato Chiba and Georgi S. Medvedev. "The mean field analysis of the kuramoto model on graphs II. asymptotic stability of the incoherent state, center manifold reduction, and bifurcations". In: *Discrete &; Continuous Dynamical Systems - A* 39.7 (2019), pp. 3897–3921.

[17] Luigi Ambrosio, Nicola Gigli, and Giuseppe Savaré. *Gradient flows: in metric spaces and in the space of probability measures*. Springer, 2005.

A Conditions on intersection between a rectangular hyperbola and the unit circle

The problem of finding the zeros of the velocity field is equivalent to finding the points of intersection between the unit circle $C_1 \equiv x^2 + y^2 - 1 = 0$ and the rectangular hyperbola $H_1 \equiv ax + by - 2xy = 0$. This motivates us to obtain conditions on the parameters a, b that guarantee C_1 and H_1 intersect at two, three or four intersections points. This classification is provided in the following lemma.

Lemma A.0.1. Let n denote the number of intersection points between C_1 and H_1, then the following statements follow

- $n = 2$ iff either $a^{2/3} + b^{2/3} > 2^{2/3}, (a, b) \neq (0, 0)$ or $|a| \geq 2, b = 0$ or $|b| \geq 2, a = 0$
- $n = 3$ iff $a^{2/3} + b^{2/3} = 2^{2/3}, (a, b) \neq (0, 0)$
- $n = 4$ iff $a^{2/3} + b^{2/3} < 2^{2/3}, (a, b) \neq (0, 0)$ or or $|a| < 2, b = 0$ or $|b| < 2, a = 0$.

Proof. The conics C_1, H_1 have the following homogeneous matrix representations $C_1 \equiv z^\top C z = 0, H_1 = z^\top H z = 0$, where

$$C = \begin{bmatrix} 1 & 0 & 0 \\ 0 & 1 & 0 \\ 0 & 0 & -1 \end{bmatrix}, H = \begin{bmatrix} 0 & -1 & a/2 \\ -1 & 0 & b/2 \\ a/2 & b/2 & 0 \end{bmatrix}$$

and $z = [x, y, 1]^\top$ is the homogeneous coordinates. The pencil of conics formed by C_1, H_1, are given by

$$C(\lambda, \mu) = \lambda C_1 + \mu H_1$$

To obtain the points of intersection we seek to find a (perhaps many) suitable (λ^*, μ^*) such that $C(\lambda^*, \mu^*)$ is degenerate. Such a degenerate $C(\lambda^*, \mu^*)$ would be given by a pair of straight lines. The points of intersection of each straight line with conics C_1 or H_1 would coincide with the points of intersection between C_1 and H_1. The value of (λ^*, μ^*) can be obtained by setting $\det\left(\lambda C_1 + \mu H_1\right) = 0$. This results in the following depressed cubic equation in (λ^*, μ^*)

$$\lambda^3 - \lambda\mu^2\left(1 - \frac{a^2 + b^2}{4}\right) + \mu^3 \frac{ab}{2} = 0. \tag{43}$$

We proceed one case at a time,

- If $(a, b) = (0, 0)$, then (43) simplifies to $\lambda^3 - \lambda\mu^2 = 0$, therefore $\lambda^* = 0$ or $\lambda^* = \pm\mu^*$. Substituting these back, $C(\lambda^*, \mu^*) \equiv (x - y + 1)(x - y - 1) = 0$. Intersecting these lines with the circle C_1 we obtain the points $(\pm 1, 0), (0, \pm 1)$. Therefore we have four intersections points.
- If $a \neq 0, b = 0$, then (43) simplifies to $\lambda^3 - \lambda\mu^2(1 - a^2/4) = 0$. We have the following sub-cases as well
  - If $|a| < 2$, then $\lambda^* = 0$ or $\lambda^* = \pm\mu\sqrt{1 - a^2/4}$. Substituting these back we obtain $C(\lambda^*, \mu^*) = x(a - 2y) = 0$. Intersecting these lines with the circle C_1, we obtain the points $(\pm 1, 0), (\pm\sqrt{1 - a^2/4}, a/2)$. Therefore, we have four points of intersection.
  - If $|a| \geq 2$ then $\lambda^* = 0$ is the only solution, therefore we get $C(0, \mu^*) \equiv x(a - 2y) = 0$. Intersecting with C_1, we obtain the points $(\pm 1, 0)$. Therefore we only have two points of intersection.
- If $a = 0, b \neq 0$. As the problem is symmetric in a and b, the analysis is the same as $a \neq 0, b = 0$. We have the following sub-cases
  - If $|b| < 2$, then we have four points of intersection given by $(0, \pm 1), (b/2, \pm\sqrt{1 - b^2/4})$.
  - If $|b| \geq 2$, then $(0, \pm 1)$ are the only two points of intersection.
- If $(a, b) \neq (0, 0)$, then λ^* and μ^* cannot be simultaneously zero (this would render $C(\lambda^* + \mu^*)$ degenerate but with no useful information). Therefore, we can divide (43) by μ^3 to obtain the depressed cubic in $\bar{\lambda} = \lambda/\mu$ as

  $$\bar{\lambda}^3 - \bar{\lambda}\left(1 - \frac{a^2 + b^2}{4}\right) + \frac{ab}{2} = 0. \tag{44}$$

  The number of real zeros of the cubic polynomial (44) determines the number of intersection points between C_1 and H_1. The discriminant of the cubic (44) is given by

  $$\bar{D}(a, b) = 4\left(1 - \frac{a^2 + b^2}{4}\right)^3 - 27\left(\frac{ab}{2}\right)^2$$

If $D(a,b) > 0$, then (44) has three distinct real roots, then C_1 and H_1 have four points of intersection. If $D(a,b) = 0$, then (44) has three real roots, with two repeated roots then C_1 and H_1 intersect in exactly three points (note that C_1 and H_1 still intersect in four points, with two points being the same, resulting in three distinct points of intersection). If $D(a,b) < 0$, then (44) has exactly one real root, and C_1 and H_1 have exactly two points of intersection. To obtain the conditions given in the lemma, we simplify $\bar{D}(a,b)$ further. The equation $D(a,b) = 0$ can be simplified as

$$\left(4 - (a^2 + b^2)\right)^3 = 27 \times 4(ab)^2$$

We can see that

$$\begin{aligned} D(2\cos^3(\phi), 2\sin^3(\phi)) &= 4\Big[\left(1 - \cos^6(\phi) - \sin^6(\phi)\right)^3 - 27\left(\cos^6(\phi)\sin^6(\phi)\right)^2\Big] \\ &= 4\Big[\left(1 - \cos^6(\phi) - \sin^6(\phi)\right)^3 - \left(3\cos^2(\phi)\sin^2(\phi)\right)^3\Big] \\ &= 4\left[1 - \cos^6(\phi) - \sin^6(\phi) - 3\cos^2(\phi)\sin^2(\phi)\right](\dots) \\ &= 4\left[1 - \left(\cos^2(\phi) + \sin^2(\phi)\right)^3\right](\dots) = 0 \end{aligned}$$

Therefore, $D(a,b) = 0$ is equivalent to $a^{2/3} + b^{2/3} = 2^{2/3}$.

The statement of the lemma follows and this concludes the proof. ■

B Proof of Theorem 11

The simplest perturbation is the constant perturbation $p(x) \equiv p$. Applying this perturbation to the quadratic form (39), terms cancel, and we obtain

$$\left(\int 2K_s \cos(2\theta(x))\, dx\right) p^2. \tag{45}$$

For this quantity to be ≥ 0 for all p requires that

$$\int \cos(2\theta(x))\, dx \;\geq\; 0. \tag{46}$$

We interpret this condition as expressing that "the values in θ (equivalently, the mass in ρ) must be concentrated sufficiently near the minima of the second harmonic injection $-\cos(2\theta)$, i.e., sufficiently near $\{0, \pi\}$."

For our next perturbation, we take $p = \pm I(w, \epsilon)$, a positive or negative indicator function on an ϵ neighborhood of the point $w \in [0,1]$. This perturbation is a proxy for a perturbation of a single oscillator. Note that θ can be taken to be piecewise constant, since it must be valued in the zero set of v_θ, which is discrete. Applying this perturbation to the quadratic form (39), we obtain

$$\epsilon\left(2K_s\cos(2\theta(w)) - K\int \cos(\theta(w) - \theta(y))\, dy\right) + K\epsilon^2. \tag{47}$$

For small ϵ, clearly only the term in parentheses matters. We recognize this term as the negative gradient of the velocity field v_θ evaluated at $\theta(w)$. Thus, these perturbations are destabilizing if $\theta(w)$ is an unstable zero of v_θ, that is, if $\nabla v_\theta(w) > 0$.

Thus, candidate stable equilibria θ must be valued in the set of stable zeros of v almost everywhere (equivalently, ρ must be supported on the set of stable zeros). Based on the analysis in Section 3.4, we know that v can have

exactly 2, 3, or 4 zeros. By standard topological arguments, the continuity of v allows us to conclude that v must have exactly 1 or 2 stable zeros. Thus, we may now restrict our attention to candidate stable equilibria θ having just one or two levels (equivalently, ρ having just one or two discrete components). We consider these cases separately in the following two subsections.

B.1 Single-Level Case

In the case where θ has a single level (equivalently, ρ has a single mass), we take $\theta(x) \equiv \theta$. We evaluate the dynamics (7) to find that the interaction term vanishes, and are left with

$$\dot{\theta} \;=\; -K_s \sin(2\theta). \tag{48}$$

We can see that these dynamics admit four possible equilibria at 0, $\pi/2$, π, and $3\pi/2$. Applying the test (46) allows us to rule out the equilibria at $\pi/2$ and $3\pi/2$, leaving only those at 0 and π as candidate stable equilibria.

B.2 Double-Level Case

We now consider the case where θ has two levels: $\theta(x) = \theta_1$ on $[0, m)$ and $\theta(x) = \theta_2$ on $(m, 1]$. We assume that we are *genuinely* in a two-mass case here (i.e. that $m \notin \{0, 1\}$, $\theta_1 \neq \theta_2$) since the single-mass case has already been treated above.

Both θ_1 and θ_2 must be valued in the set of stable zeros of v, and by the intersection of conics argument given in Section 3.4, if there are two distinct stable zeros of v, these must exist in separate halves of the unit circle: one in $(3\pi/2, \pi/2)$ and one in $(\pi/2, 3\pi/2)$. Without loss of generality, we may assume that $\theta_1 \in (3\pi/2, \pi/2)$ and $\theta_2 \in (\pi/2, 3\pi/2)$.

Evaluating the resulting dynamics (7) for each level, we obtain

$$\dot{\theta}_1 \;=\; K(1-m)\sin(\theta_1 - \theta_2) - K_s \sin(2\theta_1) \tag{49}$$

$$\dot{\theta}_2 \;=\; Km \sin(\theta_2 - \theta_1) - K_s \sin(2\theta_2). \tag{50}$$

By our earlier symmetry arguments in Section 3.3, we may equivalently consider the normalized dynamics

$$\dot{\tilde{\theta}}_1 \;=\; A(1-m)\sin(\theta_1 - \theta_2) - \sin(2\theta_1) \tag{51}$$

$$\dot{\tilde{\theta}}_2 \;=\; Am \sin(\theta_2 - \theta_1) - \sin(2\theta_2), \tag{52}$$

where $A := K/K_s$.

The equilibrium condition here is that both of the terms above be zero simultaneously. This also means that any linear combination of these terms must be zero. For example, scaling the two equations by m and $1-m$ and summing them, we obtain the condition

$$m\sin(2\theta_1) + (1-m)\sin(2\theta_2) \;=\; 0. \tag{53}$$

Similarly, considering the difference of the two terms, we obtain

$$A\sin(\theta_1 - \theta_2) - \sin(2\theta_1) + \sin(2\theta_2) \;=\; 0, \tag{54}$$

which can be simplified (using the difference of sines formula) to

$$\sin(\theta_1 - \theta_2)(A - 2\cos(\theta_1 + \theta_2)) \;=\; 0. \tag{55}$$

In particular, either $\sin(\theta_1 - \theta_2) = 0$, or $A - 2\cos(\theta_1 + \theta_2) = 0$. If $\sin(\theta_1 - \theta_2) = 0$, then since we are assuming $\theta_1 \neq \theta_2$, θ_1 and θ_2 must differ by π. Considering the dynamics (51)-(52) implies that $\sin(2\theta_1) = \sin(2\theta_2) = 0$, and thus either $\{\theta_1, \theta_2\} = \{0, \pi\}$ or $\{\theta_1, \theta_2\} = \{\pi/2, 3\pi/2\}$. The latter case is ruled out by our earlier assumptions on θ_1, θ_2 (or by the test (46)), leaving $\{\theta_1, \theta_2\} = \{0, \pi\}$ as the only candidate equilibria if $\sin(\theta_1 - \theta_2) = 0$. Thus, in what follows, we may assume that $A - 2\cos(\theta_1 + \theta_2) = 0$.

For these equilibria to be stable, it is necessary that the Jacobian matrix

$$J \;=\; \begin{bmatrix} A(1-m)\cos(\theta_1 - \theta_2) - 2\cos(2\theta_1) & -A(1-m)\cos(\theta_1 - \theta_2) \\ -Am\cos(\theta_1 - \theta_2) & Am\cos(\theta_1 - \theta_2) - 2\cos(2\theta_2) \end{bmatrix} \tag{56}$$

be negative semidefinite. This means that $x^T J x \leq 0$ for all $x \in \mathbb{R}^2$, or equivalently, that

$$x_1^2\left[A(1-m)\cos(\theta_1 - \theta_2) - 2\cos(2\theta_1)\right] + x_1 x_2\left[-A\cos(\theta_1 - \theta_2)\right] + x_2^2\left[Am\cos(\theta_1 - \theta_2) - 2\cos(2\theta_2)\right] \;\leq\; 0 \tag{57}$$

for all $x_1, x_2 \in \mathbb{R}$. Any choice of x_1, x_2 gives a necessary condition for stability here. Taking $x_1 = 1 + \epsilon_1$, $x_2 = -1 + \epsilon_2$, for example, we obtain

$$\begin{aligned}\left[2A\cos(\theta_1 - \theta_2) - 2\cos(2\theta_1) - 2\cos(2\theta_2)\right] + \epsilon_1\left[A(3-2m)\cos(\theta_1 - \theta_2) - 4\cos(2\theta_1)\right] \\ - \epsilon_2\left[A(1+2m)\cos(\theta_1 - \theta_2) - 4\cos(2\theta_2)\right] + o(\epsilon) \;\leq\; 0.\end{aligned} \tag{58}$$

The first term (which is not multiplied by an ϵ) can be simplified using the sum of cosines formula to

$$2\cos(\theta_1 - \theta_2)(A - 2\cos(\theta_1 + \theta_2)), \tag{59}$$

which is zero, since $A - 2\cos(\theta_1 + \theta_2) = 0$ from earlier. Thus, there exist some ϵ_1, ϵ_2 such that the inequality is violated unless both terms multiplying ϵ_1, ϵ_2 are identically zero, that is,

$$A(3-2m)\cos(\theta_1 - \theta_2) - 4\cos(2\theta_1) \;=\; 0 \tag{60}$$

$$A(1+2m)\cos(\theta_1 - \theta_2) - 4\cos(2\theta_2) \;=\; 0. \tag{61}$$

Similarly to before, any linear combination of these terms must be zero. Multiplying the first term by $(1+2m)$ and the second by $(3-2m)$ and taking the difference gives

$$-(1+2m)\cos(2\theta_1) + (3-2m)\cos(2\theta_2) \;=\; 0. \tag{62}$$

Any possible stable equilibria in this case must satisfy this equation together with (53):

$$m\sin(2\theta_1) + (1-m)\sin(2\theta_2) \;=\; 0. \tag{63}$$

Applying the identities

$$\sin(2\theta_1) \;=\; \sin((\theta_1 + \theta_2) + (\theta_1 - \theta_2)) \;=\; \sin(\theta_1 + \theta_2)\cos(\theta_1 - \theta_2) + \cos(\theta_1 + \theta_2)\sin(\theta_1 - \theta_2) \tag{64}$$

and similarly for cos and for θ_2, we obtain the system

$$\begin{bmatrix} \cos(\theta_1 - \theta_2) & (2m-1)\sin(\theta_1 - \theta_2) \\ 4\sin(\theta_1 - \theta_2) & -2(2m-1)\cos(\theta_1 - \theta_2) \end{bmatrix} \begin{bmatrix} \sin(\theta_1 + \theta_2) \\ \cos(\theta_1 + \theta_2) \end{bmatrix} \;=\; \begin{bmatrix} 0 \\ 0 \end{bmatrix}. \tag{65}$$

This system has a solution if and only if the determinant of the matrix is zero, since $\sin(\theta_1+\theta_2)$ and $\cos(\theta_1+\theta_2)$ cannot simultaneously be 0, that is, if

$$-2(2m-1)\cos^2(\theta_1-\theta_2) - 4(2m-1)\sin^2(\theta_1-\theta_2) \;=\; -2(2m-1)(1+\sin^2(\theta_1-\theta_2)) \;=\; 0. \tag{66}$$

Since $1+\sin^2$ is always positive, this requires that $2m-1=0$, or that $m=0.5$. Applying this to the system (65), we may conclude that $\sin(\theta_1+\theta_2)$ must be 0.

Now, this implies that either $\theta_1+\theta_2=0$ or $\theta_1+\theta_2=\pi$. By our earlier assumption that $\theta_1\in(3\pi/2,\pi/2)$, $\theta_2\in(\pi/2,3\pi/2)$, we can see that $\theta_1+\theta_2$ cannot be equal to 0, and therefore it must be equal to π. Thus, we may also conclude that $\cos(\theta_1+\theta_2)=-1$, and by our earlier condition $A-2\cos(\theta_1+\theta_2)$, that $A=-2$. The condition that $\theta_1+\theta_2=\pi$ also leads to a host of other identities, including $\sin(\theta_1)=\sin(\theta_2)$, $\cos(\theta_1)=-\cos(\theta_2)$, $\sin(\theta_1-\theta_2)=-\sin(2\theta_1)=\sin(2\theta_2)$, and $\cos(\theta_1-\theta_2)=-\cos(2\theta_1)=-\cos(2\theta_2)$.

The test (46) then allows us to further limit the possible ranges of θ_1 and θ_2 to $[7\pi/4,\pi/4]$ and $[3\pi/5,5\pi/4]$, respectively. For these equilibria ($m=0.5$, $A=-2$, θ_1,θ_2 in the given ranges, with $\theta_1+\theta_2=\pi$), the Jacobian (56) appears to only be negative semidefinite, that is, it has a zero eigenvalue. And indeed, even using higher-order stability tests, these equilibria appear to be neutrally stable.

C Proof of Theorem 12

Case 1: We begin with the case where $m=1$, i.e., where $\theta(x)=0$ on all of $[0,1]$. (The case with $m=0$ is symmetric and so has the same stability threshold.)

In this case, the quadratic form (39) simplifies to

$$\begin{aligned} D^2E(\theta)[p,p] \;&=\; (2K_s-K)\int p^2(x)\,dx + K\int p(x)p(y)\,dx\,dy && (67)\\ &=\; (2K_s-K)\|p\|_{L^2}^2 + K\left(\int p\right)^2 && (68)\\ &=\; 2K_s\|p\|_{L^2}^2 - K\left[\int p^2 - \left(\int p\right)^2\right] && (69)\\ &=\; 2K_s\|p\|_{L^2}^2 - K\mathrm{var}(p). && (70)\end{aligned}$$

We can put upper and lower bounds on the variance: $0\le\mathrm{var}(p)\le\|p\|_{L^2}^2$. These upper and lower bounds are both achieved by perturbations p which are constant and zero-mean, respectively. Thus we can obtain the following (tight) bounds on the quadratic form:

$$\begin{aligned} K \text{ positive} \quad&\Rightarrow\quad (2K_s-K)\|p\|^2 \;\le\; D^2E(\theta)[p,p] \;\le\; 2K_s\|p\|^2 && (71)\\ K \text{ negative} \quad&\Rightarrow\quad 2K_s\|p\|^2 \;\le\; D^2E(\theta)[p,p] \;\le\; (2K_s-K)\|p\|^2. && (72)\end{aligned}$$

The strongest conclusion that can be drawn here is from the lower bound when K is positive. That is, that $2K_s-K>0$ or $K/K_s<2$ is sufficient for stability. This same condition is necessary if the strict inequality is relaxed to a non-strict one, since the lower bound is achieved.

Case 2: Next, we treat the case where $m=0.5$. Using the identity $\cos(a-b)=\cos(a)\cos(b)+\sin(a)\sin(b)$, we obtain

$$D^2E(\theta)[p,p] \;=\; 2K_s\|p\|_{L^2}^2 + K\left(\int_0^{0.5}p-\int_{0.5}^1 p\right)^2 \;=\; 2K_s\|p\|_{L^2}^2 + K\left(\int p\cos(\theta)\right)^2. \tag{73}$$

Here, we use the bounds $0 \leq (\int p\cos(\theta))^2 \leq \|p\|_{L^2}^2$, which are achieved by p having the same sign and opposite sign on $[0,m)$ and $(m,1]$, respectively. Thus we get the following (tight) upper and lower bounds for the quadratic form:

$$K \text{ positive} \quad \Rightarrow \quad 2K_s\|p\|^2 \;\leq\; D^2E(\theta)[p,p] \;\leq\; (2K_s+K)\|p\|^2 \tag{74}$$

$$K \text{ negative} \quad \Rightarrow \quad (2K_s+K)\|p\|^2 \;\leq\; D^2E(\theta)[p,p] \;\leq\; 2K_s\|p\|^2. \tag{75}$$

The strongest conclusion that can be drawn here is from the lower bound when K is negative. That is, $2K_s+K>0$ or $K/K_s > -2$ is sufficient for stability. Again, this same condition is necessary if the strict inequality is relaxed to a non-strict one, since the lower bound is achieved.

Case 3: Now, we examine the case where $m \notin \{0, 0.5, 1\}$. We can use the same tricks, including the identity $\cos(a-b) = \cos(a)\cos(b)+\sin(a)\sin(b)$, to obtain

$$D^2E(\theta)[p,p] \;=\; 2K_s\|p\|_{L^2}^2 - K(2m-1)\int \cos(\theta(x))p^2(x)\,dx + K(\int \cos(\theta(x))p(x)\,dx)^2. \tag{76}$$

Naively (i.e. not considering interdependence between the terms), we can bound the middle term from above and below by $\pm K|2m-1|\|p\|^2$, and we can bound the last term from above and below by $\pm K\|p\|^2$ and 0 depending on the sign of K. This gives the following bounds on the quadratic form:

$$K \text{ positive} \quad \Rightarrow \quad (2K_s - K|2m-1|)\|p\|^2 \;\leq\; D^2E(\theta)[p,p] \;\leq\; (2K_s + K(|2m-1|+1))\|p\|^2 \tag{77}$$

$$K \text{ negative} \quad \Rightarrow \quad (2K_s + K(|2m-1|+1))\|p\|^2 \;\leq\; D^2E(\theta)[p,p] \;\leq\; (2K_s - K|2m-1|)\|p\|^2. \tag{78}$$

The strongest conclusion that can be drawn here uses both lower bounds: $2K_s - K|2m-1| > 0$ or $K/K_s < 2/|2m-1|$ is sufficient for stability if K is positive, and $2K_s + K(|2m-1|+1) > 0$ or $K/K_s > -2/(|2m-1|+1)$ is sufficient for stability if K is negative. Altogether, this gives that

$$-2/(|2m-1|+1) \;<\; K/K_s \;<\; 2/|2m-1| \tag{79}$$

is sufficient for stability. The only remaining question is whether these bounds are tight. That is, can we find a perturbation p that achieves the lower bounds for each term in (76) simultaneously? The answer is yes: If K is positive, then these bounds are achieved for p supported on $(m,1]$ if $2m-1$ is negative or on $[0,m)$ if $2m-1$ is positive, and having zero mean on that set. If K is negative, then these lower bounds are achieved for p supported on $[0,m)$ if $2m-1$ is negative or on $(m,1]$ if $2m-1$ is positive, and having a strict sign on that set. Thus, the bounds are indeed tight, and so again, this same condition is necessary if the strict inequality is relaxed to a non-strict one.